Global Journal of Science Frontier Research: A Physics and Space Science
Volume 14 Issue 6 Version 1.0 Year 2014
Type : Double Blind Peer Reviewed International Research Journal
Publisher: Global Journals Inc. (USA)
Online ISSN: 2249-4626 & Print ISSN: 0975-5896

Theory of Shubnikov-De Haas and Quantum Hall Oscillations in Graphene under Bias and Gate Voltages

By Shigeji Fujita & Akira Suzuki
State University of New York, United States

Abstract- Magnetic oscillations in graphene under gate and bias voltages, measured by Tan et al. [Phys. Rev. B **84**, 115429 (2011)] are analyzed theoretically. The Shubnikov-de Haas (SdH) oscillations occur at the lower fields while the Quantum Hall (QH) oscillations occur at the higher fields. Both SdH and QH oscillations have the same periods: $\varepsilon_{\rm F}/\hbar\omega_{\rm c}$, where $\varepsilon_{\rm F}$ is the Fermi energy and $\omega_{\rm c}$ the cyclotron frequency. Since the phases are different by $\pi/2$, transitions between the maxima and the minima occur at some magnetic field strength. A quantum statistical theory of the SdH oscillations is developed. A distinctive feature of two dimensional (2D) magnetic oscillations is the absence of the background. That is, the envelopes of the oscillations approach zero with a zero-slope central line. The amplitude of the SdH oscillations decreases like $[\sinh(2\pi^2 M^* k_{\rm B}T/\hbar eB)]^{-1}$, where M^* is the magnetotransport mass of the field-dressed electron distinct from the cyclotron mass m^* of the electron. A theory of the QHE is developed in terms of the composite (c)-bosons and c-fermions. The half-integer QHE in graphene at filling factor $\nu = (2P+1)/2$, $P = 0, \pm1, \pm2, \cdots$ arises from the Bose-Einstein condensation of the c-bosons formed by the phonon exchange between a pair of like-charge c-fermions with two fluxons.

Keywords: *Shubnikov-de Haas (SdH) oscillation, quantum Hall (QH) oscillation, 2D magnetic oscillation, composite (c-) fermion, c-boson, fluxon, Cooper pair (pairon), magnetotransport mass, cyclotron mass.*

GJSFR-A Classification : *FOR Code: 020699p*

Strictly as per the compliance and regulations of :

Theory of Shubnikov-De Haas and Quantum Hall Oscillations in Graphene under Bias and Gate Voltages

Shigeji Fujita [α] & Akira Suzuki [σ]

Abstract- Magnetic oscillations in graphene under gate and bias voltages, measured by Tan et al. [Phys. Rev. B84, 115429 (2011)] are analyzed theoretically. The Shubnikov - de Haas (SdH) oscillations occur at the lower fields while the Quantum Hall (QH) oscillations occur at the higher fields. Both SdH and QH oscillations have the same periods: $\varepsilon_{\rm F}/\hbar\omega_{\rm c}$, where $\varepsilon_{\rm F}$ is the Fermi energy and $\omega_{\rm c}$ the cyclotron frequency. Since the phases are different by π/2, transitions between the maxima and the minima occur at some magnetic field strength. A quantum statistical theory of the SdH oscillations is developed. A distinctive feature of two dimensional (2D) magnetic oscillations is the absence of the background. That is, the envelopes of the oscillations approach zero with zero-slope central line. The amplitude of the SdH oscillations decreases like $[\sinh(2\pi^2 M^* k_{\rm B}T/\hbar eB)]^{-1}$, where M^* is the magnetotransport mass of the field-dressed electron distinct from the cyclotron mass m^* of the electron. A theory of the QHE is developed in terms of the composite (c)-bosons and c-fermions. The half integer QHE in graphene at filling factor $\nu=(2P+1)/2$, $P=0,\pm1,\pm2,\cdots$ arises from the Bose-Einstein condensation of the c-bosons formed by the phonon exchange between a pair of like-charge c-fermions with two fluxons. The QH states are bound and stabilized with a superconducting energy gap. They are more difficult to destroy than the SdH states. The temperature dependence of the magnetic resistance between 2 K and 50 K is interpreted, using the population change of phonons (scatterers).

PACS numbers: 05.20.Dd, 72.80.Vp, 73.43.Qt, 73.43.-f, 73.50.Fq.

Keywords: Shubnikov-de Haas (SdH) oscillation, quantum Hall (QH) oscillation, 2D magnetic oscillation, composite (c-) fermion, c-boson, fluxon, Cooper pair (pairon), magnetotransport mass, cyclotron mass.

I. Introduction

In 2011 Tan *et al.* [1] discovered a phase inversion of the magnetic oscillations in graphene under the gate voltage $V_{\rm g}=-40$ V at 2.0 K. At lower fields ($B<2$ T) the magnetic resistance R_{xx} has a negligible dependence on dc bias while R_{xx} at higher fields show temperature - dependent damping oscillations. Their data are shown in Fig. 1. The original authors considered the Shubnikov-de Haas (SdH) oscillations only. It is more natural to interpret the data in terms of the SdH oscillations at lower fields and the quantum Hall (QH) oscillations at higher fields. The SdH oscillations originates in the sinusoidal oscillations within the drop in the Fermi distribution function of electrons (see Fig. 2). At low temperatures $(k_{\rm B}T\ll\varepsilon_{\rm F}, T\sim 2\,{\rm K})$ and low fields, where the Fermi energy $\varepsilon_{\rm F}$ is much greater than the the cyclotron frequency $\omega_{\rm c}\equiv eB/m^*$, the SdH oscillations are visible. The dc bias negligibly affects the Fermi energy $\varepsilon_{\rm F}$, and hence the resistance remains flat. A distinctive feature of 2D magnetic oscillations is the absence of the background. That is, the envelopes of the oscillations approach zero with a zero-slope central line. This feature is clearly seen in Fig. 1. Fujita and Suzuki described this feature in their book [2]. For completeness their theory is outlined in Appendix A. A theory of the SdH oscillations in 2D is given in Section II. Following Fujita and Okamura [3], we develop a quantum statistical theory of the QHE in terms of composite particles (boson, fermion) in Section III. A discussion is given in Section IV.

Author α: Department of Physics, University at Buffalo, State University of New York, Buffalo, USA. e-mail: fujita@buffalo.edu

Author σ: Department of Physics, Faculty of Science, Tokyo University of Science, Shinjyuku-ku, Tokyo, Japan.
e-mail: asuzuki@rs.kagu.tus.ac.jp

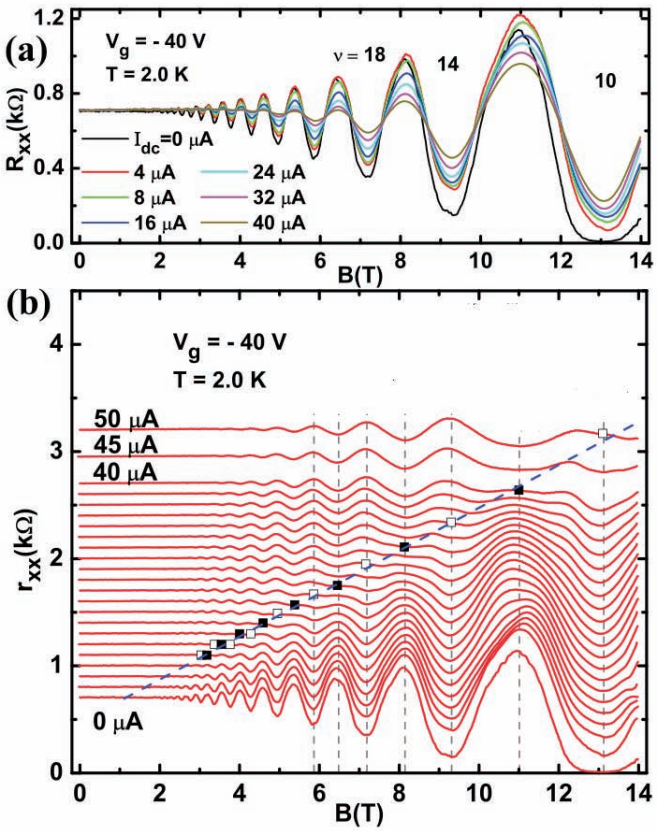

Figure 1 : (Color online) (a) The magnetic resistance R_{xx} measured at the gate voltage $V_g = -40\,\mathrm{V}$ and the temperature T∼2.0 K at various bias-induced currents. (b) The differential magnetic resistance r_{xx}. The inversion is marked by vertical dash lines (after Tan *et al.* [1]).

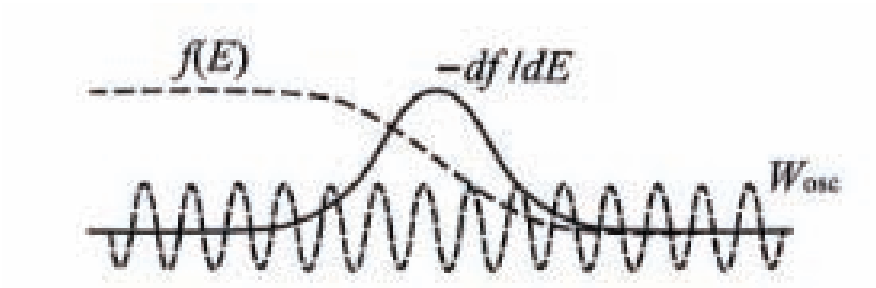

Figure 2 : Numerous oscillations in $\mathcal{W}_{\mathrm{osc}}$ within the width of $-\mathrm{d}f/\mathrm{d}\varepsilon$ generates SdH oscillations.

II. Shubnikov-De Haas Oscillations

Oscillations in magnetoresistance (MR), similar to the de Haas-van Alphen (dHvA) oscillations in the magnetic susceptibility, were first observed by Shubnikov and de Haas in 1930 [4]. These oscillations are often called the SdH oscillations. The susceptibility is an equilibrium property and can therefore be calculated by standard statistical mechanical methods. The MR is a non-equilibrium property, and its treatment requires a kinetic theory. The magnetic oscillations in both cases arise from the periodically varying density of states for the electrons subjected to magnetic fields. We shall see that the observation of the oscillations gives a direct measurement of the *magnetotransport mass* M^*. The observation also gives the quantitative information on the *cyclotron mass* m^*.

Let us take a system of electrons moving in a plane. Applying a magnetic field $\boldsymbol{B}$ perpendicular to the plane, each electron will be in the Landau state with the energy ε:

$$\varepsilon = \left(N_{\rm L} + \frac{1}{2}\right)\hbar\omega_{\rm c}, \quad \omega_{\rm c} \equiv \frac{eB}{m^*}, \quad N_{\rm L} = 0, 1, 2, \ \ldots \quad (1)$$

The degeneracy of the Landau level (LL) is given by

$$\frac{eBA}{2\pi\hbar}, \qquad A = \text{sample area.} \quad (2)$$

The weaker is the field, the more LL's, separated by $\hbar\omega_{\rm c}$, are occupied by the electrons. In this Landau state the electron can be viewed as circulating around the guiding center. The radius of circulation $l \equiv (\hbar/eB)^{1/2}$ for the Landau ground state is about 250 Å at a field B = 1.0 T (tesla). If we now apply a weak electric field E, then the guiding center jumps and generates a current.

Let us first consider the case with no magnetic field. We assume a uniform distribution of impurities with the density $n_{\rm I}$. Solving the Boltzmann equation, we obtain the conductivity:

$$\sigma = \frac{e^2}{m^*} n\tau = \frac{2e^2}{m^*(2\pi\hbar)^2} \int {\rm d}^2p \, \frac{\varepsilon}{\Gamma} \left(-\frac{{\rm d}f}{{\rm d}\varepsilon}\right), \quad \varepsilon = \frac{p^2}{2m^*}, \quad (3)$$

where n = electron density, and Γ is the energy (ε)-dependent relaxation rate:

$$\Gamma(\varepsilon) = n_{\rm I} \int {\rm d}\Omega \left(\frac{p}{m^*}\right) I(p, \theta)(1 - \cos\theta), \quad (4)$$

where θ = scattering angle and $I(p, \theta)$ = scattering cross-section, and the Fermi distribution function:

$$f(\varepsilon) \equiv \frac{1}{e^{\beta(\varepsilon - \mu)} + 1} \quad (5)$$

with $\beta \equiv (k_{\rm B}T)^{-1}$ and μ = chemical potential, is normalized such that

$$n = \frac{2}{(2\pi\hbar)^2} \int {\rm d}^2p \, f(\varepsilon), \quad (6)$$

where the factor 2 is due to the spin degeneracy. We introduce the density of states, $\mathcal{D}(\varepsilon)$, such that

$$\frac{2}{(2\pi\hbar)^2} \int {\rm d}^2p \, \cdots = \int {\rm d}\varepsilon \, \mathcal{D}(\varepsilon) \, \cdots \, . \quad (7)$$

We can then rewrite Eq.(3) as

$$\sigma = \frac{e^2}{m^*} \int_0^\infty {\rm d}\varepsilon \, \mathcal{D}(\varepsilon) \, \frac{\varepsilon}{\Gamma} \left(-\frac{{\rm d}f}{{\rm d}\varepsilon}\right). \quad (8)$$

The Fermi distribution function $f(\varepsilon)$ drops steeply near $\varepsilon = \mu$ at low temperatures:

$$k_{\rm B}T \ll \varepsilon_{\rm F}. \quad (9)$$

The density of states, $\mathcal{D}(\varepsilon)$, is a slowly varying function of the energy ε. For a 2D free electron system, the density of states is independent of the energy ε. Then the Dirac delta-function replacement formula

$$-\frac{{\rm d}f}{{\rm d}\varepsilon} = \delta(\varepsilon - \mu) \quad (10)$$

can be used. Assuming this formula, using

$$\int_0^\infty {\rm d}\varepsilon \, \mathcal{D}(\varepsilon) \, \varepsilon \left(-\frac{{\rm d}f}{{\rm d}\varepsilon}\right) = \int_0^\infty {\rm d}\varepsilon \, \mathcal{D}(\varepsilon) \, f(\varepsilon), \quad (11)$$

and comparing Eq. (3) and Eq. (8), we obtain

$$\tau = \int_0^\infty {\rm d}\varepsilon \, \mathcal{D}(\varepsilon) \, \frac{1}{\Gamma(\varepsilon)} \, f(\varepsilon) \quad (12)$$

for the relaxation time τ. The temperature dependence of τ is introduced through the Fermi distribution function $f(\varepsilon)$.

Next we consider the case with a magnetic field. A classical electron spirals around the applied static magnetic field $\boldsymbol{B}$. The guiding center motion generates an electric current. The spiraling state has a lower energy than the straight line motion state since the current runs in a diamagnetic manner.

Following Onsager [5], we assume that the magnetic field magnitude B is quantized such that

$$B = n_\phi \Phi_0, \quad n_\phi \equiv \frac{N_\phi}{A}, \quad \Phi_0 = \frac{e}{\hbar}, \quad (13)$$

where N_ϕ is the number of *elementary fluxes (fluxons)*. Following Jain [6], we introduce field-dressed (attached) electrons, which can move straight in all directions (isotropically) in the absence of an electric field. The dressed electron by assumption has a charge magnitude e and a magnetotransport mass M^* distinct from the cyclotron mass m^*. Applying kinetic theory to the motion of the dressed electrons, we shall obtain the conductivity formula

$$\sigma = e^2 n\tau/M^* \,. \tag{14}$$

We introduce *kinetic momenta* $\boldsymbol{\Pi}$:

$$\Pi_x \equiv p_x + eA_x \,, \quad \Pi_y \equiv p_y + eA_y \,. \tag{15}$$

The kinetic energy is

$$\mathcal{H}_{\rm K} = \frac{1}{2M^*}(\Pi_x^2 + \Pi_y^2) \equiv \frac{1}{2M^*}\Pi^2 \,. \tag{16}$$

After simple calculations, we obtain

$$\mathrm{d}x\mathrm{d}\Pi_x\mathrm{d}y\mathrm{d}\Pi_y \equiv \mathrm{d}x\mathrm{d}p_x\mathrm{d}y\mathrm{d}p_y \,. \tag{17}$$

We can now represent quantum states by the quasi-phase space elements $\mathrm{d}x\mathrm{d}\Pi_x\mathrm{d}y\mathrm{d}\Pi_y$. The Hamiltonian $\mathcal{H}$ in Eq. (16) does not depend on the position (x, y). Assuming large

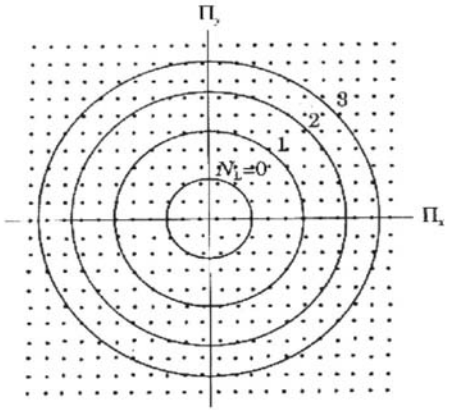

Figure 3 : The 2D Landau states are represented by the circular shells in the $\Pi_x\Pi_y$ -space.

normalization lengths (L_x, L_y), $A = L_xL_y$, we can then represent the Landau states by the concentric shells in the $\Pi_x\Pi_y$ -space (see Fig. 3), having the statistical weight

$$\frac{2\pi L_xL_y}{(2\pi\hbar)^2}\Pi\Delta\Pi = \frac{A}{2\pi\hbar}\omega_c m^* = \frac{eAB}{2\pi\hbar} \tag{18}$$

with the energy separation $\hbar\omega_c = \Delta(\Pi^2/2m^*) = \Pi\Delta\Pi/m^*$. Equations (18) confirm that the LL degeneracy is $eBA/(2\pi\hbar)$ as stated in Eq. (2).

Let us introduce a distribution function $\varphi(\boldsymbol{\Pi}, t)$ in the $\Pi_x\Pi_y$ -space normalized such that

$$\frac{2}{(2\pi\hbar)^2}\int \mathrm{d}^2\,\Pi\ \varphi(\Pi_x, \Pi_y, t) = \frac{N}{A} = n \,. \tag{19}$$

The Boltzmann equation for a homogeneous stationary system is

$$e(\boldsymbol{E} + \boldsymbol{v}\times\boldsymbol{B})\cdot\frac{\partial\varphi}{\partial\boldsymbol{\Pi}} = \int \mathrm{d}\Omega\,\frac{\Pi}{M^*}\,n_{\rm I}\,I(\Pi,\theta)\,[\varphi(\boldsymbol{\Pi}') - \varphi(\boldsymbol{\Pi})] \,, \tag{20}$$

where θ is the angle of deflection, that is, the angle between the initial and final kinetic momenta $(\boldsymbol{\Pi}, \boldsymbol{\Pi}')$. In the actual experimental condition the magnetic force term can be neglected. Assuming this condition, we obtain the same Boltzmann equation as that for a field-free system. Hence, we obtain the conductivity formula (14) (with m^* being replaced by M^*).

As the field B is raised, the separation $\hbar\omega_c$ becomes greater and the quantum states are bunched together. The density of states should contain an oscillatory part:

$$\sin\left(\frac{2\pi\varepsilon'}{\hbar\omega_c} + \phi_0\right) \,, \qquad \varepsilon' = \frac{\Pi'^2}{2m^*} \,, \tag{21}$$

where ϕ_0 is a phase. Since

$$\varepsilon_{\rm F}/\hbar\omega_c \gg 1 \qquad (\text{weak field}) \,, \tag{22}$$

the phase ϕ_0 will be dropped hereafter. Physically, the sinusoidal variations in Eq. (21) arise as follows. From the Heisenberg uncertainty principle and the Pauli exclusion principle, the Fermi energy $\varepsilon_{\rm F}$ remains approximately constant as the field B varies. The density of states is high when $\varepsilon_{\rm F}$ matches the $N_{\rm L}$-th level, while it is small when $\varepsilon_{\rm F}$ falls between neighboring LL's.

If the density of states, $\mathcal{D}(\varepsilon)$, oscillates violently in the drop of the Fermi distribution function $f(\varepsilon) \equiv [e^{\beta(\varepsilon-\mu)} + 1]^{-1}$, one cannot use the delta function replacement formula in Eq. (10). The use of Eq. (10) is limited to the case in which the integrand is a smooth function near $\varepsilon = \mu$. The width of $|\mathrm{d}f/\mathrm{d}\varepsilon|$ is of the order $k_{\rm B}T$. The critical temperature T_c below which the oscillations can be observed is $k_{\rm B}T_c \sim \hbar\omega_c$. Below the critical temperature, $T < T_c$, we may proceed as follows. Let us consider the integral

$$I = \int_0^\infty \mathrm{d}\varepsilon\, f(\varepsilon)\,\sin\left(\frac{2\pi\varepsilon}{\hbar\omega_c}\right) \qquad \varepsilon \equiv \frac{\Pi^2}{2M^*} \,. \tag{23}$$

For temperatures satisfying $\beta\varepsilon = \varepsilon/k_{\rm B}T \gg 1$, we obtain straightforwardly

$$I = \pi k_{\rm B}T \frac{\cos(2\pi\varepsilon_{\rm F}/\hbar\omega_{\rm c})}{\sinh(2\pi^2 M^* k_{\rm B}T/\hbar eB)}\,. \qquad (24)$$

Here we used

$$M^*\mu(T=0) = m^*\varepsilon_{\rm F} = \frac{1}{2}\,p_{\rm F}^2\,, \qquad (25)$$

which follows from the fact that the Fermi momentum $p_{\rm F}$ is the same for both dressed and undressed electrons. The mathematical steps going from Eq. (23) to Eq. (24) are given in Appendix B.

In summary, (i) the SdH oscillation period is $\varepsilon_{\rm F}/\hbar\omega_{\rm c}$. This arises from the bunching of the quantum states. (ii) The amplitude of the oscillations exponentially decreases like $[\sinh(2\pi^2 M^* k_{\rm B}T/\hbar eB)]^{-1}$. Thus, if the "decay rate" δ defined through

$$\sinh\left(\frac{\delta}{B}\right) \equiv \sinh\left(\frac{2\pi^2 M^* k_{\rm B}T}{\hbar eB}\right) \qquad (26)$$

is measured carefully, the magnetotransport mass M^* can be obtained *directly* through $M^* = e\hbar\delta/(2\pi^2 k_{\rm B}T)$. This finding is important. For example, the relaxation rate τ^{-1} can now be obtained through the conductivity formula (14) with the measured magnetoconductivity.

All electrons, not just those excited electrons near the Fermi surface, are subject to the $\boldsymbol{E}$-field. Hence, the carrier density n appearing in Eq. (14) is the *total* density of the dressed electrons. This *n* also appears in the Hall resistivity expression:

$$\rho_{\rm H} \equiv \frac{E_{\rm H}}{j} = \frac{v_{\rm d}B}{env_{\rm d}} = \frac{B}{en}\,, \qquad (27)$$

where the Hall effect condition $E_{\rm H} = v_{\rm d}B$, $v_{\rm d}$ = drift velocity, was used.

In the *cyclotron motion* the electron with the cyclotron mass m^* circulates around the magnetic field. Hence, the cyclotron frequency $\omega_{\rm c}$ is given by eB/m^*. The guiding center (dressed electron) moves with the magnetotransport mass M^*, whence this M^* appears in the hyperbolicsine term in Eq. (24).

In 1952 Dingle [7] developed a theory of the dHvA oscillations. He proposed to explain the envelope behavior in terms of a Dingle temperature $T_{\rm D}$ such that the exponential decay factor be

$$\exp\left[\frac{-\lambda(T+T_{\rm D})}{B}\right], \qquad \lambda = \text{constant}. \qquad (28)$$

Instead of the Dingle temperature, we introduced the magnetotransport mass M^* to explain the envelope behavior. The susceptibility χ is an equilibrium property, and hence, χ can be calculated without considering the relaxation mechanism. In our theory, the envelope of the oscillations is obtained by taking the average of the sinusoidal density of states with the Fermi distribution of the dressed electrons. There is no place where the impurities come into play. The validity of our theory may be checked by varying the impurity density. Our theory predicts little change in the clearly defined envelope.

The SdH oscillations are a fermionic phenomenon while the QH oscillations are a bosonic one with a superconducting energy gap, which will be discussed in the following section.

III. Fractinal Quantum Hall Effect

The fractional QHE can be treated in terms of composite (c-) particles (boson, fermion). The c-boson (c-fermion), each containing an electron and an odd (even) number of fluxons, were introduced by Zhang *et al*. [8] and Jain [6] for the description of the fractional QHE (Fermi liquid).

There is a remarkable similarity between the QHE *and* the High-Temperature Superconductivity (HTSC), both occurring in two-dimensional (2D) systems as pointed out by Laughlin [9]. We regard the *phonon exchange attraction* as the causes of both QHE and HTSC. Starting with a reasonable Hamiltonian, we calculate everything, using quantum statistical method.

The countability concept of the fluxons, known as the *flux quantization*:

$$B = \frac{N_\phi}{A}\frac{h}{e} \equiv n_\phi \frac{h}{e}\,, \qquad (29)$$

where N_ϕ = fluxon number (integer) and h = Planck constant, is originally due to Onsager [5]. The magnetic (electric) field is an axial (polar) vector and the associated fluxon (photon) is a half-spin fermion (full-spin boson). The magnetic (electric) flux line cannot (can) terminate at a sink, which supports the fermionic (bosonic) nature of the fluxon (photon). No half-spin fermion can annihilate itself because of angular momentum conservation. The electron spin originates in the relativistic quantum equation (Dirac's theory of electron) [10]. The discrete (two) quantum numbers ($\sigma_z = \pm 1$) cannot change in the continuous limit, and hence the spin must be conserved. The countability and statistics of the fluxon are fundamental particle properties. We postulate that *the fluxon is a half-spin fermion with zero mass and zero charge*. Fluxons are similar to neutrinos. The fluxon (neutrino) occurs in electron (nucleon) dynamics. Hence fluxon and neutrino are regarded as distinct from each other.

The Center-of-Mass (CM) of *any* c-particle moves as a fermion or a boson. The eigenvalues of the CM momentum are limited to 0 or 1 (unlimited) if it contains an odd (even) number of elementary fermions. This rule is known as the *Ehrenfest-Oppenheimer-Bethe's (EOB's) rule* [11]. Hence the CM motion of the composite containing an electron and Q fluxons is bosonic (fermonic) if Q is odd (even). The system of c-bosons condenses below some critical temperature $T_{\rm c}$

and exhibits a superconducting state while the system of c-fermions shows a Fermi liquid behavior.

A longitudinal phonon, acoustic or optical, generates a density wave, which affects the electron (fluxon) motion through the charge displacement (current). The exchange of a phonon between electrons and fluxons can generate an *attractive* transition, see below.

Bardeen, Cooper and Schrieffer (BCS) [12] assumed the existence of Cooper pairs [13] in a superconductor, and wrote down a Hamiltonian containing the "electron" and "hole" kinetic energies and the pairing interaction Hamiltonian with the phonon variables eliminated. We start with a BCS-like Hamiltonian $\mathcal{H}$ for the QHE[3]:

$$\mathcal{H}=\sum_{\boldsymbol{k}}{}'\sum_{s}\varepsilon^{(1)}_{\boldsymbol{k}}n^{(1)}_{\boldsymbol{k}s}+\sum_{\boldsymbol{k}}{}'\sum_{s}\varepsilon^{(2)}_{\boldsymbol{k}}n^{(2)}_{\boldsymbol{k}s}+\sum_{\boldsymbol{k}}{}'\sum_{s}\varepsilon^{(3)}_{\boldsymbol{k}}n^{(3)}_{\boldsymbol{k}s}$$
$$-\sum_{\boldsymbol{q}}{}'\sum_{\boldsymbol{k}}{}'\sum_{\boldsymbol{k}'}{}'\sum_{s}v_0\left[B^{(1)\dagger}_{\boldsymbol{k}'\boldsymbol{q}\,s}B^{(1)}_{\boldsymbol{k}\boldsymbol{q}\,s}+B^{(1)\dagger}_{\boldsymbol{k}'\boldsymbol{q}\,s}B^{(2)\dagger}_{\boldsymbol{k}\boldsymbol{q}\,s}+B^{(2)}_{\boldsymbol{k}'\boldsymbol{q}\,s}B^{(1)}_{\boldsymbol{k}\boldsymbol{q}\,s}+B^{(2)}_{\boldsymbol{k}'\boldsymbol{q}\,s}B^{(2)\dagger}_{\boldsymbol{k}\boldsymbol{q}\,s}\right], \tag{30}$$

where

$$n^{(j)}_{\boldsymbol{k}s}=c^{(j)\dagger}_{\boldsymbol{k}s}c^{(j)}_{\boldsymbol{k}s} \tag{31}$$

is the number operator for the "electrons" (1) ["holes" (2), fluxon (3)] at momentum $\boldsymbol{k}$ and spin s with the energy $\varepsilon^{(j)}_{\boldsymbol{k}}$, with annihilation (creation) operators $c\ (c^{\dagger})$ satisfying the Fermi anti-commutation rules:

$$\{c^{(i)}_{\boldsymbol{k}s},\,c^{(j)\dagger}_{\boldsymbol{k}'s'}\}\equiv c^{(i)}_{\boldsymbol{k}s}c^{(j)\dagger}_{\boldsymbol{k}'s'}+c^{(j)\dagger}_{\boldsymbol{k}'s'}c^{(i)}_{\boldsymbol{k}s}=\delta_{\boldsymbol{k},\boldsymbol{k}'}\delta_{s,s'}\delta_{i,j}\,,\quad \{c^{(i)}_{\boldsymbol{k}s},c^{(j)}_{\boldsymbol{k}'s'}\}=0\,. \tag{32}$$

The fluxon number operator $n^{(3)}_{\boldsymbol{k}s}$ is represented by $a^{\dagger}_{\boldsymbol{k}s}a_{\boldsymbol{k}s}$ with $a\ (a^{\dagger})$ satisfying the anticommutation rules:

$$\{a_{\boldsymbol{k}s},\,a^{\dagger}_{\boldsymbol{k}'s'}\}=\delta_{\boldsymbol{k},\boldsymbol{k}'}\delta_{s,s'}\,,\quad \{a_{\boldsymbol{k}s},\,a_{\boldsymbol{k}'s'}\}=0\,. \tag{33}$$

The phonon exchange attraction can create electron-fluxon composites. We call the conduction-electron composite with an odd (even) number of fluxons c-boson (c-fermion). The electron (hole)-type c-particles carry negative (positive) charge. The pair operators B in Eq. (30) are defined by

$$B^{(1)\dagger}_{\boldsymbol{k}\boldsymbol{q},s}\equiv c^{(1)\dagger}_{\boldsymbol{k}+\boldsymbol{q}/2,s}a^{\dagger}_{-\boldsymbol{k}+\boldsymbol{q}/2,-s}\,,\quad B^{(2)}_{\boldsymbol{k}\boldsymbol{q},s}\equiv a_{-\boldsymbol{k}+\boldsymbol{q}/2,-s}c^{(2)}_{\boldsymbol{k}+\boldsymbol{q}/2,s}\,. \tag{34}$$

The prime on the summation in Eq. (30) means the restriction:

$$0<\varepsilon^{(j)}_{\boldsymbol{k}s}<\hbar\omega_{\mathrm{D}}\,,\quad \omega_{\mathrm{D}}=\text{the Debye frequency}. \tag{35}$$

The pairing interaction terms in Eq. (30) conserve the charge. The term $-v_0B^{(1)\dagger}_{\boldsymbol{k}'\boldsymbol{q}\,s}B^{(1)}_{\boldsymbol{k}\boldsymbol{q}\,s}$, where $v_0\equiv|V_{\boldsymbol{q}}V'_{\boldsymbol{q}}|\,(\hbar\omega_0A)^{-1}$, is the pairing strength, generates a transition in electron-type c-fermion states. Similarly, the exchange of a phonon generates a transition between hole-type c-fermion states, represented by $-v_0B^{(2)\dagger}_{\boldsymbol{k}'\boldsymbol{q}\,s}B^{(2)\dagger}_{\boldsymbol{k}\boldsymbol{q}\,s}$. The phonon exchange can also pair-create (pair-annihilate) electron (hole) type-c-boson pairs, and the effects of these processes are represented by $-v_0B^{(1)\dagger}_{\boldsymbol{k}'\boldsymbol{q}\,s}B^{(2)\dagger}_{\boldsymbol{k}\boldsymbol{q}\,s}\ \left(-v_0B^{(1)}_{\boldsymbol{k}\boldsymbol{q}\,s}B^{(2)}_{\boldsymbol{k}\boldsymbol{q}\,s}\right)$.

The Cooper pair is formed from two "electrons" (or "holes"). Likewise the c-bosons may be formed by the phonon-exchange attraction from c-fermions and fluxons. If the density of the c-bosons is high enough, then the c-bosons will be Bose-Einstein (BE)-condensed and exhibit a superconductivity.

To treat superconductivity we may modify the pair operators in Eq. (34) as

$$B^{(1)\dagger}_{\boldsymbol{k}\boldsymbol{q},s}\equiv c^{(1)\dagger}_{\boldsymbol{k}+\boldsymbol{q}/2,s}c^{(1)\dagger}_{-\boldsymbol{k}+\boldsymbol{q}/2,-s}\,,\quad B^{(2)}_{\boldsymbol{k}\boldsymbol{q},s}\equiv c^{(2)}_{-\boldsymbol{k}+\boldsymbol{q}/2,-s}c^{(2)}_{\boldsymbol{k}+\boldsymbol{q}/2,s}\,. \tag{36}$$

Then, the pairing interaction terms in Eq. (30) are formally identical with those in the generalized BCS Hamiltonian [3]. If we assume that only zero momentum Cooper pairs ($q=0$) are generated, then the Hamiltonian $\mathcal{H}$ in Eq. (30) is reduced to the original BCS Hamiltonian, ref. [12], Eq. (2.14).

We first consider the integer QHE. We choose a conduction electron and a fluxon for the pair. The c-bosons, having the linear dispersion relation:

$$\varepsilon^{(j)} = w_0 + \frac{2}{\pi} v^{(j)} p\,, \qquad (37)$$

can move in all directions in the plane with the constant speed $(2/\pi)v_{\rm F}^{(j)}$. A brief derivation of Eq. (37) is given in Appendix C. The supercurrent is generated by $\mp$c-bosons monochromatically condensed at the momentum $\boldsymbol{p}$, running along the sample length. The supercurrent density (magnitude) j, calculated by the rule: $j =$ (carrier charge e^*)$\times$(carrier density n_0)$\times$ (drift velocity $v_{\rm d}$), is given by

$$j \equiv e^* n_0 v_{\rm d} = e^* n_0 \frac{2}{\pi} \left| v_{\rm F}^{(1)} - v_{\rm F}^{(2)} \right| . \qquad (38)$$

The Hall field (magnitude) $E_{\rm H}$ equals $v_{\rm d}B$. The magnetic flux is quantized:

$$B = n_\phi \Phi_0\,, \quad \Phi_0 \equiv e/h\,, \qquad (39)$$

where $n_\phi \equiv N_\phi/A$ is the fluxon density. Hence the Hall resistivity $\rho_{\rm H}$ is given by

$$\rho_{\rm H} \equiv \frac{E_{\rm H}}{j} = \frac{v_{\rm d}B}{e^* n_0 v_{\rm d}} = \frac{1}{e^* n_0} n_\phi \left(\frac{h}{e}\right) = h/e^2\,. \qquad (40)$$

Here we assumed that the c-fermion has a charge magnitude e. For the integer QHE, $e^* = e, n_\phi = n_0$, thus we obtain $\rho_{\rm H} = h/e^2$, the correct plateau value observed for the principal $\rm QHE$ at $\nu = 1$.

The supercurrent generated by equal numbers of $\mp$c-bosons condensed monochromatically is neutral. This is reflected in our calculations in Eq. (40). In the calculation we used the *unaveraged* drift velocity difference $(2/\pi)|v_{\rm F}^{(1)} - v_{\rm F}^{(2)}|$, which is significant. *Only* the unaveraged drift velocity $v_{\rm d}$ cancels out exactly from numerator/denominator, leading to an exceedingly accurate plateau value.

We now extend our theory to include elementary fermions (electron, fluxon) as members of the c-fermion set. We can then treat the QHE and the HTSC in a unified manner by using the same Hamiltonian $\mathcal{H}$.

We assume that *any c-fermion has the effective charge e^* equal to the electron charge (magnitude) e:*

$$e^* = e \quad \text{for } \textit{any} \text{ c-fermion.} \qquad (41)$$

After studying the low-field QH states of c-fermions, we obtain

$$n_\phi^{(Q)} = n_{\rm e}/Q, \quad Q = 2,\, 4, \cdots\,, \qquad (42)$$

for the density of the c-fermions with Q fluxons, where $n_{\rm e}$ is the electron density. All fermionic QH states (points) lie on the classical-Hall-effect straight line passing the origin with a constant slope when $\sigma_{\rm H}$ is plotted as a function of B^{-1}. The density $n_\phi^{(Q)}$ is proportional to the magnetic field B. As the magnetic field is raised, the separation between the LL becomes greater. The higher-Q c-fermion is more difficult to form energetically. This condition is unlikely to depend on the statistics of the c-particles. Hence Eq. (42) should be valid for all integers, odd or even.

$$n_\phi^{(Q)} = n_{\rm e}/Q\,, \quad Q = 1,\, 2, \cdots\,, \qquad (43)$$

We take the case of $Q = 3$. The c-boson containing an electron and three fluxons can be formed from a c-fermion with two fluxons and a fluxon. If the c-bosons are BE-condensed, then the supercurrent density *j* is given by Eq. (38). Hence we obtain

$$\rho_{\rm H} \equiv \frac{E_{\rm H}}{j} = \frac{v_{\rm d}B}{e^* n_0 v_{\rm d}} = \frac{n_\phi}{e^* n_0} \left(\frac{h}{e}\right) = \frac{1}{3}\frac{h}{e^2}\,, \qquad (44)$$

where we used Eqs. (41) and (43).

The principal fractional QHE occurs at $\nu = 1/3$, where the Hall resistivity value is $h/(3e^2)$ as shown in Eq. (44). A set of weaker QHE occur on the lower field side at

$$\nu = \frac{1}{3},\, \frac{2}{3},\, \cdots\,. \qquad (45)$$

The QHE behavior at $\nu = P/Q$ for any Q is similar. We illustrate it by taking integer QHE with $\nu = P$ $(= 1,\, 2, \cdots)$. The field magnitude becomes smaller with increasing P. The $\rm LL$ degeneracy is proportional to B, and hence P $\rm LL$'s must be considered. First consider the case $P = 2$. Without the phonon-exchange attraction the electrons occupy the lowest two LL's with spin. See Fig. 4 (a). The electrons at each level form c-bosons.

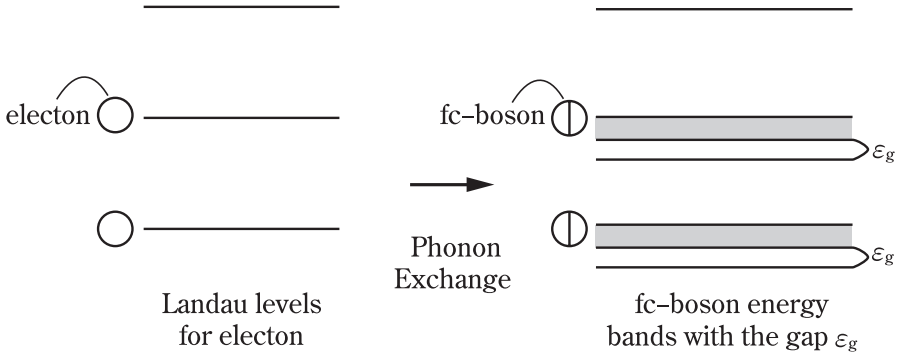

Figure 4 : The electrons which fill up the lowest two LL's, shown in (a) form the QH state at $\nu = 2$ in (b) after the phonon-exchange attraction and the BEC of the c-bosons.

In the superconducting state the supercondensate occupy the monochromatically condensed state, which is separated by the superconducting gap ε_g from the continuum states (band) as shown in the right-hand figure in Fig. 4 (b). The temperature-dependent energy gap $\varepsilon_g(T)$ is defined in terms of the BCS energy parameter Δ. A brief discussion of $\varepsilon_g(T)$ is given in Appendix D. The c-boson density n_0 at each LL is one-half the c-boson density at $\nu = 1$, which is equal to the electron density n_e fixed for the sample. Extending the theory to a general integer, we have

$$n_0 = n_e/P\,. \tag{46}$$

The critical temperature T_c for the condensed c- bosons, which is derived in Appendix E, is given by

$$T_c = 1.24\,\hbar v_F k_B^{-1} n_0^{1/2}\,, \quad n_0 \equiv N_0/A\,, \tag{47}$$

and the gap energy ε_g are smaller for higher P, making the plateau width (a measure of ε_g) smaller in agreement with experiments. The c-bosons have lower energies than the conduction electrons. Hence at the extreme low temperatures the supercurrent due to the condensed c-bosons dominates the normal current due to the conduction electrons and non-condensed c-bosons, giving rise to the dip in ρ.

The main advantages of the c-particles theory are:

- Laughlin's idea of fractional charges of the elementary excitations [14] are not required.
- The c-particles theory indicates that the strength of the QHE is greater at ν = 1/3, 1/5, $\cdots$ in the descending order than at ν = 1 as seen in the experiments [15].
- The half-integer QHE for graphene can be described simply, which will be discussed in Section IV(a).

IV. Discussion

a) Half-integer QHE

The QHE in graphene is observed at filling factor

$$\nu = \frac{2P+1}{2}\,, \quad P = 0,\, \pm 1,\, \pm 2, \cdots\,. \tag{48}$$

The half-integer QHE arises from the BEC of the c-bosons formed by the phonon exchange between a pair of like-charge (simplest) c-fermions with two fluxons. This can be seen by calculating the Hall resistivity ρ_H as follows:

We assume that any c-fermion has the effective charge $e^* = e$ for any c-fermion. After studying the weak-field fermionic QH states we obtain

$$n_\phi^{(Q)} = n_e/Q \tag{49}$$

for the density of the c-fermions with Q fluxons. We calculate the Hall conductivity σ_H and obtain

$$\sigma_H \equiv \rho_H^{-1} = \frac{j}{E_H} = \frac{2en_0 v_d}{v_d n_\phi \Phi_0} = \frac{2e^2}{h}\,. \tag{50}$$

b) The SdH Oscillations

The QHE states with integers P= 1, 2, $\cdots$ are generated on the weaker field side. Their strength decreases with increasing P. Thus, we have obtained the rule (48) within the framework of the c-particles theory. The period of the sinusoidal oscillations is

$$\frac{\varepsilon_F}{\hbar\omega_c} \quad \text{for SdH oscillations.} \tag{51}$$

The numerous oscillations in the density of states within the width of $|-\mathrm{d}f/\mathrm{d}\varepsilon|$ generate SdH oscillations, see Fig. 2. This is caused by c-fermions with two fluxons in the low fields. The c-fermions are bound and stable. The cyclotron mass m^* and the magnetotransport mass M^* are introduced for the cyclotron motion and the guiding-center (c-fermion) motion, respectively. Careful analysis of the data can yield the values of m^* and M^*.

c) The QH Oscillations

The c-boson in graphene is formed by the phonon exchange from a pair of like charge c-fermions.

When ± c-bosons are generated abundantly in the system, they undergo a BE condensation and generate a superconducting state with an energy gap ε_g. The signature of the BE condensation is zero resistance, see Fig. 1, $\nu = 10$. The superconducting state with the energy gap is very stable. The rise in R_{xx} and r_{xx} on both sides are of an Arhenius exponential type. The period of the sinusoidal oscillations are

$$\frac{\varepsilon_F}{\hbar\omega_c} \text{ for QH oscillations.} \qquad (52)$$

Thus, the SdH and QH periods match with each other, see Eqs. (A11) and (B4). But the phases are different by $\pi/2$. This causes transitions between the oscillation maxima and minima.

d) The Gate Field Effect

Graphene and carbon nanotubes are often subjected to the so-called gate voltage in experiments. The gate voltage polarizes the conductor and the surface charges ("electrons","holes") are induced. An explanation is given in Appendix F.

The data by Tan *et al*., ref. 1, Fig. 3, are reproduced in Fig. 5. If the bias voltage is applied, then "holes" will be generated at the boundary surface and move. Only "holes" are induced on the metallic surface. The "hole" currents are normal and obey Ohm's law. Thus, the currents in μA at $V_g = -40$ V, $T = 2.0$ K are proportional to the bias voltages.

e) The Temperatures-dependent Relaxation Rate

Tan *et al.* [1] investigated the temperature dependence of the magnetic resistance between 2 and 50 K, at $V_g = -40$ V, $n = 3.16 \times 10^{12}$cm^{-2}. Their data, ref. 1, Fig. 3 are reproduced in Fig. 5. They interpreted their data, shown in Fig. 5 in terms of the elevated electron temperature. A more natural interpretation is the phonon population change. The surface "holes" are scattered by phonons populated following Planck's distribution function:

$$f(\hbar sp) = \frac{1}{e^{\beta\hbar sp} - 1}, \quad \beta \equiv (k_B T)^{-1}, \qquad (53)$$

where s is the phonon speed and p the momentum magnitude. The high-temperature limit

$$f \propto T, \quad T \to \infty \qquad (54)$$

generates

$$\gamma \equiv \tau^{-1} \propto f \propto T \qquad (55)$$

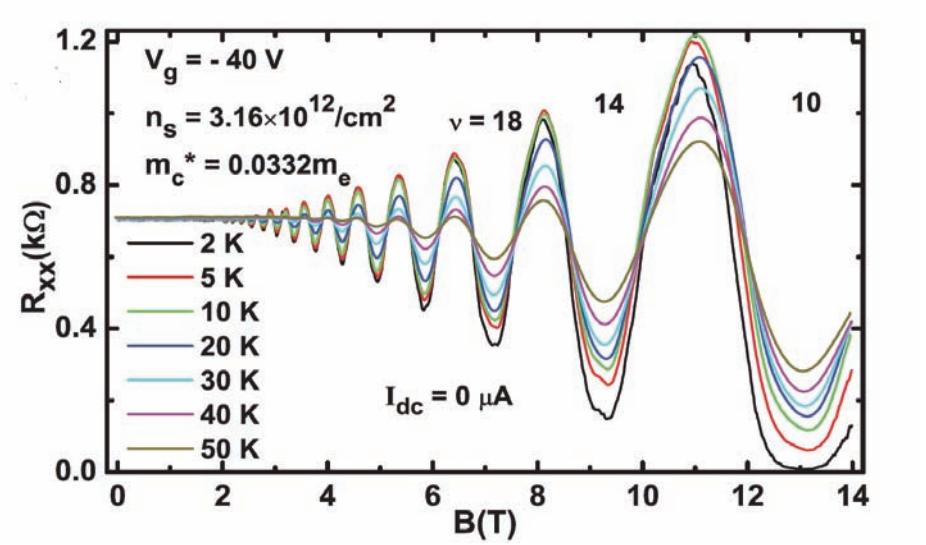

Figure 5 : (Color online) Temperature dependence of the magnetic resistance R_{xx} measured at $V_g = -40$ V and zero bias (after Tan *et al.* [1]).

for the relaxation rate $\gamma \equiv \tau^{-1}$, which is proportional to the phonon population *f*.

The highlights of the present work are:

- There are no backgrounds for both SdH and QHE oscillations, confirming that graphene is a 2D system.
- For both SdH and QH oscillations the periods of the sinusoidal oscillation are the same: $\varepsilon_F/\hbar\omega_c$.
- The SdH states are described by c-fermions with even numbers of fluxons. The c-fermions are in the negative-energy (bound) states relative to the Fermi energy.
- The QH states are described by BE-condensed c-bosons with odd numbers of fluxons. These c-bosons are in the negative-energy states and are more stable with the superconducting energy gaps ε_g.
- The envelope of the SdH oscillations decreases like $[\sinh(2\pi^2 M^* k_B T/\hbar eB)]^{-1}$ with the magnetotransport mass M^* distinct from the cyclotron mass m^* when plotted as a function of B^{-1}. The envelope grows.
- The envelope of the QH oscillations also grows and ends with the principal QHE at $\nu = \pm 1/2$. The half-

integer QH plateaus arise from the BEC of the c-bosons formed, each from a pair of like-charge c-fermions with two fluxons.

- The full set of half-integer QHE is given by $\nu = (2P + 1)/2$, $P = 0, 1, 2, \cdots$. The weaker QHE occurs on the smaller field magnitude side. The strength (width) decreases with increasing P.

V. Appendix A: Magnetic Oscillations in 2D

The statistical weight $\mathcal{W}$ is the total number of states having energies less than $\varepsilon = \left(N_{\rm L} + \frac{1}{2}\right)\hbar\omega_{\rm c}$ This $\mathcal{W}$ is given by

$$\mathcal{W} = \frac{L_x L_y}{(2\pi\hbar)^2} 2\pi\Pi\Delta\Pi \cdot 2\sum_{N_{\rm L}}^{\infty} \Theta\left[\varepsilon - \left(N_{\rm L} + \frac{1}{2}\right)\hbar\omega_{\rm c}\right], \tag{A1}$$

where $\Theta(x)$ is the Heaviside step function:

$$\Theta(x) = \begin{cases} 1 & \text{if } x > 0\,, \\ 0 & \text{if } x < 0\,. \end{cases} \tag{A2}$$

We introduce the dimensionless variable $\varepsilon^* \equiv 2\pi\varepsilon/\hbar\omega_{\rm c}$, and rewrite $\mathcal{W}$ as

$$\mathcal{W}(\varepsilon) = C\,(\hbar\omega_{\rm c})\,2\sum_{N_{\rm L}=0}^{\infty}\Theta(\varepsilon^* - (2N_{\rm L}+1)\pi)\,, \quad C \equiv 2\pi m^* A(2\pi\hbar)^{-2}\,. \tag{A3}$$

We assume a high Fermi degeneracy such that

$$\mu \simeq \varepsilon_{\rm F} \gg \hbar\omega_{\rm c}\,. \tag{A4}$$

The sum in Eq. (A3) can be computed by using Poisson's summation formula:[16]

$$\sum_{n=-\infty}^{\infty} f(2\pi n) = \frac{1}{2\pi}\sum_{n=-\infty}^{\infty}\int_{-\infty}^{\infty} {\rm d}\tau\, f(\tau)e^{-in\tau}\,. \tag{A5}$$

We write the sum in Eq. (A3) as

$$2\sum_{n=0}^{\infty}\Theta(\varepsilon - (2n+1)\pi) = \Theta(\varepsilon - \pi) + \psi(\varepsilon; 0), \tag{A6}$$

$$\psi(\varepsilon; x) \equiv \sum_{n=-\infty}^{\infty}\Theta(\varepsilon - \pi - 2\pi|n + x|)\,. \tag{A7}$$

Note that $\psi(\varepsilon; x)$ is periodic in x and can therefore be expanded in a Fourier series. After the Fourier expansion, we set $x = 0$ and obtain Eq. (A6). By taking the real part ($\mathcal{R}e$) of Eq. (A6) and using Eq. (A5), we obtain

$$\mathcal{R}e\{\text{Eq. (A6)}\} = \frac{1}{\pi}\int_0^{\infty}{\rm d}\tau\Theta(\varepsilon - \tau) + \frac{2}{\pi}\sum_{\nu=1}^{\infty}(-1)^{\nu}\int_0^{\infty}{\rm d}\tau\Theta(\varepsilon - \tau)\cos\nu\tau\,, \tag{A8}$$

where we used $\varepsilon \equiv 2\pi\varepsilon/\hbar\omega_{\rm c} \gg 1$ and neglected π against ε. The integral in the first term in Eq. (A8) yields ε. The integral in the second term is

$$\int_0^{\infty}{\rm d}\tau\,\Theta(\varepsilon - \tau)\cos\nu\tau = \frac{1}{\nu}\sin\nu\varepsilon\,. \tag{A9}$$

Thus, we obtain

$$\mathcal{R}e\{\text{Eq. (A5)}\} = \frac{1}{\pi}\varepsilon + \frac{2}{\pi}\sum_{\nu=1}^{\infty}\frac{(-1)^{\nu}}{\nu}\sin\nu\varepsilon\,. \tag{A10}$$

Using Eqs. (A3) and (A10), we obtain

$$\begin{aligned}\mathcal{W}(E) &= \mathcal{W}_0 + \mathcal{W}_{\rm osc} \\ &= C(\hbar\omega_{\rm c})\left(\frac{\varepsilon}{\pi}\right) + C\hbar\omega_{\rm c}\frac{2}{\pi}\sum_{\nu=1}^{\infty}\frac{(-1)^{\nu}}{\nu}\sin\left(\frac{2\pi\nu\varepsilon}{\hbar\omega_{\rm c}}\right)\,.\end{aligned} \tag{A11}$$

The B-independent term $\mathcal{W}_0$ is the statistical weight for the system with no fields. The term $\mathcal{W}_{\rm osc}$ generates magnetic oscillations. There is no term proportional to B^2, generating the Landau diamagnetism.

VI. Appendix B: Proof of Eq. (24)

We consider the integral:

$$\int_0^\infty \mathrm{d}\varepsilon \frac{\mathrm{d}f}{\mathrm{d}\varepsilon} \int_0^\varepsilon \mathrm{d}\varepsilon' \sin\left(\frac{2\pi\varepsilon'}{\hbar\omega_\mathrm{c}}\right) = \int_0^\infty \mathrm{d}\varepsilon \sin\left(\frac{2\pi\varepsilon}{\hbar\omega_\mathrm{c}}\right) f(\varepsilon) \equiv I\,. \tag{B1}$$

We introduce a new variable $\zeta{=}\beta(\varepsilon-\mu)$ and extend the lower limit to $-\infty\,(\beta\mu\to\infty)$, and obtain

$$\int_0^\infty \mathrm{d}\varepsilon \cdots \frac{1}{e^{\beta(\varepsilon-\mu)}+1} = \beta^{-1}\int_{-\mu\beta}^\infty \mathrm{d}\zeta \cdots \frac{1}{e^\zeta+1} \to \beta^{-1}\int_{-\infty}^\infty \mathrm{d}\zeta \cdots \frac{1}{e^\zeta+1}\,. \tag{B2}$$

Using sin(A + B) = sin A cos B + cos A sin B and

$$\int_{-\infty}^\infty \mathrm{d}\zeta\, e^{i\alpha\zeta}\frac{1}{e^\zeta+1} = \frac{\pi}{i\sinh\pi\alpha}\,, \tag{B3}$$

we obtain from Eq. (23)

$$I = \int_0^\infty \mathrm{d}\varepsilon\, f(\varepsilon)\sin\left(\frac{2\pi\varepsilon}{\hbar\omega_\mathrm{c}}\right) = \pi k_\mathrm{B}T\frac{\cos(2\pi\varepsilon_\mathrm{F}/\hbar\omega_\mathrm{c})}{\sinh(2\pi^2 M^* k_\mathrm{B}T/\hbar eB)} \tag{B4}$$

for $\varepsilon_\mathrm{F}\gg k_\mathrm{B}T$.

VII. Appendix C: Derivation of Eq. (37)

The phonon exchange attraction is in action for any pair of electrons near the Fermi surface. In general the bound pair has a net momentum, and hence, it moves. Such a pair is called a *moving pairon*. The energy w_q of a moving pairon for 2D case can be obtained from the Cooper equation [13]:

$$w_q a(\boldsymbol{k},\boldsymbol{q})\{\varepsilon(|\boldsymbol{k}+\boldsymbol{q}/2|)+\varepsilon(|-\boldsymbol{k}+\boldsymbol{q}/2|)\}a(\boldsymbol{k},\boldsymbol{q}) - \frac{v_0}{(2\pi\hbar)^2}\int' \mathrm{d}^2k'\, a(\boldsymbol{k}',\boldsymbol{q}), \tag{C1}$$

The prime on the k'-integral means the restriction on the integration domain arising from the phonon exchange attraction, see below. We note that the net momentum $\boldsymbol{q}$ is a constant of motion, which arises from the fact that the phonon exchange is an internal process, and hence cannot change the net momentum. The *pair wave functions* $a(\boldsymbol{k},\boldsymbol{q})$ are coupled with respect to the other variable $\boldsymbol{k}$, meaning that the exact (or energy-eigenstate) pairon wavefunctions are superpositions of the pair wavefunctions $a(\boldsymbol{k},\boldsymbol{q})$.

Eq. (C1) can be solved as follows. We assume that the energy w_q is negative: $w_q<0$. Then,

$$\varepsilon(|\boldsymbol{k}+\boldsymbol{q}/2|)+\varepsilon(|-\boldsymbol{k}+\boldsymbol{q}/2|)-w_q>0\,.$$

Rearranging the terms in Eq. (C1) and dividing by $\varepsilon(|\boldsymbol{k}+\boldsymbol{q}/2|)+\varepsilon(|-\boldsymbol{k}+\boldsymbol{q}/2|)-w_q$, we obtain

$$a(\boldsymbol{k},\,\boldsymbol{q}) = C(\boldsymbol{q})/\{\varepsilon(|\boldsymbol{k}+\boldsymbol{q}/2|)+\varepsilon(|-\boldsymbol{k}+\boldsymbol{q}/2|)-w_q\}\,, \tag{C2}$$

where

$$C(\boldsymbol{q}) \equiv \frac{v_0}{(2\pi\hbar)^2}\int' \mathrm{d}^2k'\, a(\boldsymbol{k}',\boldsymbol{q})\,, \tag{C3}$$

which is *k*-independent. Introducing Eq. (C2) in Eq. (C1), and dropping the common factor $C(\boldsymbol{q})$, we obtain

$$1 = \frac{v_0}{(2\pi\hbar)^2}\int' \frac{\mathrm{d}^2k}{\varepsilon(|\boldsymbol{k}+\boldsymbol{q}/2|)+\varepsilon(|-\boldsymbol{k}+\boldsymbol{q}/2|)+|w_q|}\,. \tag{C4}$$

We now assume a free-electron model. The Fermi surface is a circle of the radius (momentum)

$$k_\mathrm{F} \equiv (2m_1\varepsilon_\mathrm{F})^{1/2}\,, \tag{C5}$$

where m_1 represents the effective mass of an electron. The energy $\varepsilon(|\boldsymbol{k}|)$ is given by

$$\varepsilon(|\boldsymbol{k}|) \equiv \varepsilon_k = \frac{k^2-k_\mathrm{F}^2}{2m_1}\,. \tag{C6}$$

The prime on the k-integral in Eq. (C4) means the restriction:

$$0 < \varepsilon(|\boldsymbol{k}+\boldsymbol{q}/2|),\ \varepsilon(|-\boldsymbol{k}+\boldsymbol{q}/2|) < \hbar\omega_{\rm D}\,. \quad \text{(C7)}$$

We may choose the z-axis along $\boldsymbol{q}$ as shown in Fig. 6. The k-integral can then be expressed

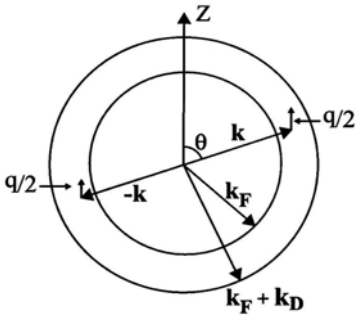

Figure 6 : The range of the interaction variables k, θ is limited to a circular shell of thickness $k_{\rm D}$

by

$$\frac{(2\pi\hbar)^2}{v_0} = 2\int_0^{\frac{\pi}{2}} {\rm d}\theta \int_{k_{\rm F}+\frac{1}{2}q\cos\theta}^{k_{\rm F}+k_{\rm D}-\frac{1}{2}q\cos\theta} \frac{k{\rm d}k}{|w_q| + 2\varepsilon_k + (4m_1)^{-1}q^2}\,, \quad \text{(C8)}$$

where $k_{\rm D}$ is given by

$$k_{\rm D} \equiv m_1\hbar\omega_{\rm D}k_{\rm F}^{-1}\,. \quad \text{(C9)}$$

After performing the integration and taking the small-q and small-$(k_{\rm D}/k_{\rm F})$ limits, we obtain

$$w_q = w_0 + \frac{2}{\pi}v_{\rm F}q\,, \quad \text{(C10)}$$

where w_0 is given by

$$w_0 = \frac{-2\hbar\omega_{\rm D}}{\exp\{2/v_0\mathcal{D}(0)\}-1}\,. \quad \text{(C11)}$$

As expected, the zero-momentum pairon has the lowest energy. The excitation energy is continuous with *no* energy gap. The energy w_q increases *linearly* with momentum q $(=|\boldsymbol{q}|)$ for small q. This behavior arises from the fact that the density-of-states is strongly reduced by increasing momentum q and dominates the q^2 increase of the kinetic energy. The linear dispersion relation means that a *Cooper pair (pairon) moves like a massless particle with a common speed* $(2/\pi)v_{\rm F}$. This relation plays a vital role in the BE condensation of pairons.

VIII. Appendix D: Temperature Dependent Energy Gap $\varepsilon_{\rm g}(T)$

The c-bosons can be bound by the interaction Hamiltonian $-v_0\,B^{(j)\dagger}_{\boldsymbol{k'q}}\,B^{(j)}_{\boldsymbol{kq}}$. The fundamental c-bosons (fc-bosons) can undergo a Bose-Einstein condensation (BEC) below the critical temperature $T_{\rm c}$. The fc-bosons are condensed at a momentum along the sample length. Above $T_{\rm c}$, they can move in all directions in the plane with the Fermi speed $v_{\rm F}^{(j)}$. The ground state energy w_0 can be calculated by solving the Cooper-like equation [13]:

$$w_0\Psi(\boldsymbol{k}) = \varepsilon_{\boldsymbol{k}}\Psi(\boldsymbol{k}) - \frac{v_0}{(2\pi\hbar)^2}\int' {\rm d}^2k'\Psi(\boldsymbol{k}')\,, \quad \text{(D1)}$$

where Ψ is the reduced wave function for the stationary fc-bosons; we neglected the fluxon energy. We obtain after simple calculations

$$w_0 = \frac{-\hbar\omega_{\rm D}}{\exp\{1/(v_0\mathcal{D}_0)\}-1} < 0\,, \quad \text{(D2)}$$

where $\mathcal{D}_0 \equiv \mathcal{D}(\varepsilon_{\rm F})$ is the density of states per spin at $\varepsilon_{\rm F}$. Note that the binding energy $|w_0|$ does not depend on the "electron" mass. Hence, the $\pm$fc-bosons have the same energy w_0.

At 0 K only *stationary* fc-bosons are generated. The ground state energy W_0 of the system of fc-bosons is

$$W_0 = 2N_0w_0\,, \quad \text{(D3)}$$

where N_0 is the $-$ (or $+$) fc-boson number.

At a finite T there are moving (non-condensed) fc-bosons, whose energies $w_{\boldsymbol{q}}^{(j)}$ are obtained from [13]

$$w_{\boldsymbol{q}}^{(j)}\Psi(\boldsymbol{k},\boldsymbol{q}) = \varepsilon^{(j)}_{|\boldsymbol{k}+\boldsymbol{q}|}\Psi(\boldsymbol{k},\boldsymbol{q}) - \frac{v_0}{(2\pi\hbar)^2}\int' {\rm d}^2k'\Psi(\boldsymbol{k}',\boldsymbol{q})\,. \quad \text{(D4)}$$

For small q, we obtain

$$w_q^{(j)} = w_0 + \frac{2}{\pi}v_{\rm F}^{(j)}|\boldsymbol{q}|\,, \quad \text{(D5)}$$

where $v_{\rm F}^{(j)} \equiv (2\varepsilon_{\rm F}/m_j)^{1/2}$ is the Fermi speed. The energy $w_q^{(j)}$ depends *linearly* on the momentum magnitude q.

The system of *free massless bosons* undergoes a BEC in 2D at the critical temperature [2]:

$$k_{\rm B}T_{\rm c} = 1.945\,\hbar c n^{1/2}\,, \qquad \text{(D6)}$$

where c is the boson speed, and n the density. The brief derivation of Eq. (D6) is given in Appendix E. Substituting $c = (2/\pi)v_{\rm F}$ in Eq. (D6), we obtain

$$k_{\rm B}T_{\rm c} = 1.24\,\hbar v_{\rm F} n_0^{1/2}\,, \qquad n_0 \equiv N_0/A\,. \qquad \text{(D7)}$$

The interboson distance $R_0 \equiv 1/\sqrt{n_0}$ calculated from this equation is $1.24\,\hbar v_{\rm F}/(k_{\rm B}T_{\rm c})$. The boson size r_0 calculated from Eq. (D7), using the uncertainty relation $q_{\max} r_0 \sim \hbar$ and $|w_0| \sim k_{\rm B}T_{\rm c}$, is $r_0 = (2/\pi)\hbar v_{\rm F}(k_{\rm B}T_{\rm c})^{-1}$, which is a few times smaller than R_0. Thus the bosons do *not* overlap in space, and the *free boson model* is justified.

Let us take GaAs/AlGaAs. We assume $m^* = 0.067 m_{\rm e}$, $m_{\rm e}$= electron mass. For the electron density 10^{11} cm^{-2}, we have $v_{\rm F} = 1.36 \times 10^6$ cm s^{-1}. Not all electrons are bound with fluxons since the simultaneous generations of $\pm$ fc-bosons is required. If we assume $n_0 = 10^{10}$ cm^{-2}, we obtain $T_{\rm c} = 1.29$ K, which is reasonable. The precise measurement of $T_{\rm c}$ may be made in a sample of constricted geometry. The plateau width should vanish at $T_{\rm c}$ since $\varepsilon_{\rm g} = 0$.

In the presence of the BE-condensate below $T_{\rm c}$ the unfluxed electron carries the energy $E_{\boldsymbol{k}}^{(j)} = \left(\varepsilon_{\boldsymbol{k}}^{(j)2} + \Delta^2\right)^{1/2}$, where the quasielectron energy gap Δ is the solution of

$$1 = v_0 \mathcal{D}_0 \int_0^{\hbar\omega_{\rm D}} {\rm d}\varepsilon \frac{1}{(\varepsilon^2+\Delta^2)^{1/2}} \left\{1 + \exp[-\beta(\varepsilon^2+\Delta^2)^{1/2}]\right\}^{-1}, \quad \beta \equiv (k_{\rm B}T)^{-1}\,. \qquad \text{(D8)}$$

Note that the gap Δ depends on T. At $T_{\rm c}$ there is *no* condensate, and hence Δ vanishes.

The *moving* fc-boson below $T_{\rm c}$ with the condensate background has the energy $\widetilde{w}_{\boldsymbol{q}}$, obtained from

$$\widetilde{w}_{\boldsymbol{q}}^{(j)} \Psi(\boldsymbol{k},\boldsymbol{q}) = E_{|\boldsymbol{k}+\boldsymbol{q}|}^{(j)} \Psi(\boldsymbol{k},\boldsymbol{q}) - \frac{v_0}{(2\pi\hbar)^2} \int' {\rm d}^2k' \Psi(\boldsymbol{k}',\boldsymbol{q})\,, \qquad \text{(D9)}$$

where $E^{(j)}$ replaced $\varepsilon^{(j)}$ in Eq. (D4). We obtain

$$\widetilde{w}_{\boldsymbol{q}}^{(j)} = \widetilde{w}_0 + \frac{2}{\pi} v_{\rm F}^{(j)} |\boldsymbol{q}| = w_0 + \varepsilon_{\rm g} + \frac{2}{\pi} v_{\rm F}^{(j)} q\,, \qquad \text{(D10)}$$

where $\widetilde{w}_0(T)$ is determined from

$$1 = \mathcal{D}_0 v_0 \int_0^{\hbar\omega_{\rm D}} \frac{{\rm d}\varepsilon}{|\widetilde{w}_0| + (\varepsilon^2+\Delta^2)^{1/2}}\,. \qquad \text{(D11)}$$

The energy difference

$$\widetilde{w}_0(T) - w_0 \equiv \varepsilon_{\rm g}(T) > 0 \qquad \text{(D12)}$$

represents the T-*dependent energy gap* between the moving and stationary fc-bosons. The energy $\widetilde{w}_{\boldsymbol{q}}$ is negative. Otherwise, the fc-boson should break up. This limits $\varepsilon_{\rm g}$ to be less than $|w_0|$. The energy gap $\varepsilon_{\rm g}(T)$ is $|w_0|$ at 0 K. It declines to zero as the temperature approaches $T_{\rm c}$.

A similar behavior also holds for graphene. The experimental electron density is 3.16 $\times 10^{12}$ cm^{-2} and the Fermi velocity $v_{\rm F} = 1.1 \times 10^6$ m/s. The critical temperature $T_{\rm c}$ is expected to be much above 300 K. The temperature 50 K can be regarded as a very low temperature relative to $T_{\rm c}$. Hence the QH state has an Arrhenius-decay type exponential stability factor:

$$\exp[-\varepsilon_{\rm g}(T=0)/k_{\rm B}T]\,, \qquad \text{(D13)}$$

where $\varepsilon_{\rm g}(T=0)$ is the zero-temperature energy gap.

IX. Appendix E: Proof of Eq. (D6)

The BEC occurs when the chemical potential μ vanishes at a finite T. The critical temperature $T_{\rm c}$ can be determined from

$$n = (2\pi\hbar)^{-2} \int {\rm d}^2p\, [e^{\beta_{\rm c}\varepsilon} - 1]^{-1}, \quad \beta_{\rm c} \equiv (k_{\rm B}T_{\rm c})^{-1}. \qquad \text{(E1)}$$

After expanding the integrand in powers of $e^{-\beta_{\rm c}\varepsilon}$ and using $\varepsilon = cp$, we obtain

$$n = 1.654\,(2\pi)^{-1}(k_{\rm B}T_{\rm c}/\hbar c)^2\,, \qquad \text{(E2)}$$

yielding formula (D6).

X. Appendix F: The Gate Field Effect

Let us take a rectangular metallic plate and place it under an external electric field $\boldsymbol{E}$, see Fig. 7. When the upper and lower sides are parallel to the field $\boldsymbol{E}$, then the remaining two sides surfaces are polarized so as to reduce the total electric field energy. If the plate is rotated, then all side surfaces are polarized.

Let us now look at the electric field effect in $\boldsymbol{k}$-space. Assume a free electron system which has a spherical Fermi surface at zero field. Upon the application of a static fielfd $\boldsymbol{E}$, the Fermi surface will be shifted towards the right by $qE\tau/m^*$, where τ is the mean free time and m^* the effective mass, as shown in Fig. 8. There is a steady current since the sphere is off

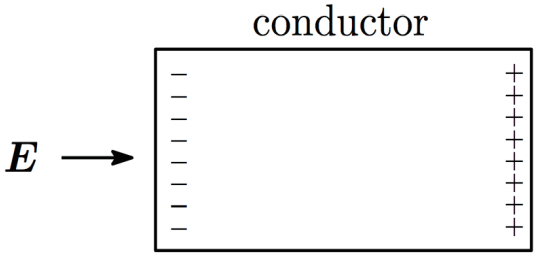

Figure 7 : The surface charges are induced in the conductor under an external electric field $\boldsymbol{E}$.

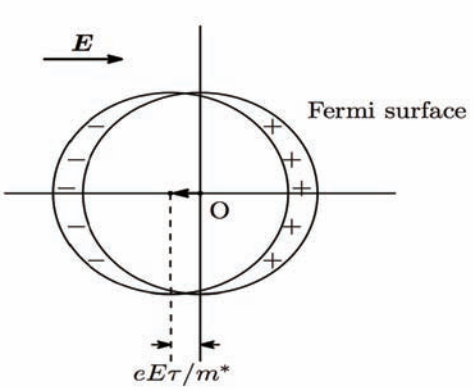

Figure 8 : The Fermi surface is shifted by $eE\tau/m^*$ due to the electric field $\boldsymbol{E}$.

from the center O. We may assume that the ionic lattice is stationary. Then, there is an unbalanced charge distribution as shown, where we assume $q = -e < 0$.

This effect will appear only on the surface of the metal. We used the fermionic nature of electrons.

REFERENCES

1. Z. Tan, C. Tan, L. Ma, G. T. Liu, L. Lu and C. L. Yang, Phys. Rev. B **84**, 115429 (2011).
2. S. Fujita and A. Suzuki, *Electrical Conduction in Graphene and Nanotubes,* (Wiley-VCH, Weinheim, Germany, 2013).
3. S. Fujita and Y. Okamura, Phys. Rev. B **69**, 155313 (2004); see also, S. Fujita, K. Ito, Y. Kumek and Y. Okamura, Phys. Rev. B **70**, 075304 (2004).
4. L. Shubnikov and W. J. de Haas, Leiden Comm. 207a, 207c, 207d, 210a (1930).
5. L. Onsager, Philos. Mag. **43**, 1006 (1952).
6. J. K. Jain, Phys. Rev. Lett. **63**, 199 (1989); Phys. Rev. B **40,** 8079 (1989); *ibid.* B **41**, 7653 (1990); Surf. Sci. **263**, 65 (1992): see also J. K. Jain, *Composite Fermions*, (Cambridge University Press, Cambridge, UK, 2007).
7. R. B. Dingle, Proc.Roy. Soc. A **211**, 500 (1952).
8. S. C. Zhang, T.H. Hansson and S. Kivelson, Phys. Rev. Lett. **62**, 82 (1989).
9. R. B. Laughlin, Science **242**, 525 (1988).
10. P. A. M. Dirac, *Principles of Quantum Mechanics*, 4th ed. (Oxford University Press, Oxford, UK, 1958), pp. 172-176, pp. 248-252, p. 267.
11. P. Ehrenfest and J. R. Oppenheimer, Phys. Rev. **37**, 311 (1931); H. A. Bethe and R. J. Jackiw, *Intermediate Quantum Mechanics*, 2nd ed., Benjamin, New York, 1968, p. 23; S. Fujita and D.L. Morabito, Mod. Phys. Lett. B **12** 1061 (1998).
12. J. Bardeen, L.N. Cooper and J. R. Schrieffer, Phys. Rev. **108**, 1175 (1957).
13. L. N. Cooper, Phys. Rev. **104**, 1189 (1956).
14. R. B. Laughlin, Phys. Rev. Lett. **50**, 1395 (1983).
15. R. G. Clark, J. R. Mallett, S. R. Haynes, J. J. Harris and C. T. Foxon, Phys. Rev. Lett. **60**, 1747 (1988); V. G. Goldman and B. Su, Science **267**, 1010 (1995); L. Saminadayar, D. C. Glattli, Y. Jin, B. Etienne, Phys. Rev. Lett. **79**, 2526 (1997); R. de Picciotto, M. Reznikov,M. Heiblum, V. Umansky, G. Bunin and D. Mahalu, Nature **389**, 162 (1997).
16. M. Stone and P. Goldbart, *Mathematics for Physics* (Cambridge University Press, Cambridge, UK, 2009), p. 792; P. M. Morse and H. Feshbach, *Methods of Theoretical Physics* (McGraw- Hill, New York, 1953), pp. 466-467; R. Courant and D. Hilbert, *Methods of Mathematical Physics*, vol. 1 (Wiley-Interscience, New York, 1953), pp.76-77.